

The segmental and chain relaxation modes in high-cis-polyisoprene as studied by thermally stimulated currents

Elsa Mora, Ana R. Brás, Wim Pyckhout-Hintzen, Hermínio P. Diogo, and Joaquim J. Moura Ramos

Citation: *The Journal of Chemical Physics* **142**, 044903 (2015); doi: 10.1063/1.4906542

View online: <http://dx.doi.org/10.1063/1.4906542>

View Table of Contents: <http://scitation.aip.org/content/aip/journal/jcp/142/4?ver=pdfcov>

Published by the [AIP Publishing](#)

Articles you may be interested in

[Effect of physical aging on the Johari-Goldstein and \$\alpha\$ relaxations of D-sorbitol: A study by thermally stimulated depolarization currents](#)

J. Chem. Phys. **126**, 144506 (2007); 10.1063/1.2722263

[Study of dielectric relaxation modes in poly\(\$\epsilon\$ -caprolactone\): Molecular weight, water sorption, and merging effects](#)

J. Chem. Phys. **114**, 6417 (2001); 10.1063/1.1355288

[Glass transition relaxation and fragility in the molecular glass forming m-toluidine: A study by thermally stimulated depolarization currents](#)

J. Chem. Phys. **113**, 3204 (2000); 10.1063/1.1286959

[Comparative study of the relaxation behavior at very low frequencies of acrylate polymers with pendant 1,3-dioxane rings in their structure](#)

J. Appl. Phys. **84**, 4436 (1998); 10.1063/1.368698

[Relaxation behavior of semiflexible polymers at very low frequencies](#)

J. Appl. Phys. **81**, 3685 (1997); 10.1063/1.364743



AIP | The Journal of
Chemical Physics

Meet The New Deputy Editors

| | | | | | |
|---|-------------------|---|------------------------------|---|-------------------------|
|  | Peter Hamm |  | David E. Manolopoulos |  | James L. Skinner |
|---|-------------------|---|------------------------------|---|-------------------------|

The segmental and chain relaxation modes in high-*cis*-polyisoprene as studied by thermally stimulated currents

Elsa Mora,¹ Ana R. Brás,² Wim Pyckhout-Hintzen,² Hermínio P. Diogo,^{1,a)}
and Joaquim J. Moura Ramos^{3,b)}

¹CQE—Centro de Química Estrutural, Universidade de Lisboa, Complexo I, IST, 1049-001 Lisboa, Portugal

²Jülich Centre for Neutron Science and Institute for Complex Systems, Forschungszentrum Jülich, 52425 Jülich, Germany

³CQFM—Centro de Química-Física Molecular and IN—Institute of Nanoscience and Nanotechnology, Instituto Superior Técnico, Universidade de Lisboa, 1049-001 Lisboa, Portugal

(Received 13 November 2014; accepted 12 January 2015; published online 28 January 2015)

The technique of Thermally Stimulated Currents is used to study the slow molecular mobility in a series of poly (1,4-*cis*-isoprene) samples with different molecular weights, M_w , and low polydispersity. The technique revealed a high resolution power, particularly useful in the study of the lower molecular weight samples where the chain and the segmental relaxations strongly overlap. The dynamic crossover that is reported for the normal mode by varying the molecular weight is clearly revealed by the thermally stimulated depolarization currents results through the temperature location, T_{Mn} , of the normal mode peak, the values of the relaxation time at T_{Mn} , $\tau(T_{Mn})$, and the value of the fragility index of the normal mode, m_n . The kinetic features of the glass transition relaxation of polyisoprene have also been determined. © 2015 AIP Publishing LLC. [<http://dx.doi.org/10.1063/1.4906542>]

I. INTRODUCTION

Among the different dielectric relaxation processes observed in polymers, some of them have frequency (or temperature) location that are almost independent of the molecular weight; this is the case for the secondary relaxations and for the main (or α -) relaxation that display the same location for M_w above a critical value. However, a small number of polymers show a higher temperature (or lower frequency) mobility, the so-called normal mode process, that occurs in polymers with a dipole moment component parallel to the chain contour: type-A polymers according to the classification of Stockmayer.¹ The phenomenology and the theory of the normal mode relaxation are described in several works, and the experimental technique most often used to study this mobility is dielectric relaxation spectroscopy (DRS).^{2–5}

Thermally Stimulated Currents (TSC) is a dielectric related experimental technique that has been extensively used in the study of slow mobility in polymers,⁶ and new contributions from this technique in this context have been recently highlighted.^{7,8} However, and surprisingly, the TSC studies on the normal mode (or chain dynamics) are extremely scarce. One of the reasons for this situation is probably due to the difficulty of using TSC to probe dipole reorientation and diffusion at temperatures above the glass transition temperature. In fact, above T_g , in the metastable liquid or rubber state, the viscosity is lower and the molecular mobility is higher; in these conditions, TSC often shows strong conductivity arising from the motion of free charge carriers, that disguises any dipolar signal eventually present above T_g . TSC is also fertile in artifacts arising from polarization due to the presence of hopping charge

carriers, or heterogeneities leading to interfacial polarization, sometimes referred to as the Maxwell-Wagner-Sillars effect. It is thus necessary to be very careful to assign the TSC relaxation signals above T_g .

Despite these difficulties, two important thermally stimulated depolarization currents (TSDC) works on the normal mode have been published very recently, both concerning *cis*-1,4-polyisoprene. One of them⁹ is focused on the specific problem of the non-exponential nature of the slower Rouse modes, while the other¹⁰ is a general TSC study of the segmental and chain dynamics. As a consequence of its molecular asymmetry, poly (1,4-*cis*-isoprene) is one of such polymers displaying the normal mode relaxation, which has been characterized in great detail by dielectric relaxation spectroscopy; among the large number of works on this subject, let us refer those by Adachi and Kotaka,^{3,11–13} Boese and Kremer,^{14–16} and Schönhals.^{17,18} Given that the normal mode mobility is fully characterized by DRS, and since this polymer is not expected to present any particular conductivity problems, we chose *cis*-polyisoprene to carry through a detailed TSC mobility study. With the obtained results, we wish to show the usefulness of TSC to study segmental and chain mobilities, and to underline the complementarity between the two dielectric techniques of TSC and DRS.

II. EXPERIMENTAL

A. Materials

Linear (predominantly *cis*) poly (1,4-isoprene), PI, samples with molecular weights, M_w , in the range 2000–550 000 g mol^{−1}, and degrees of polydispersity indexes, PDI, between 1.04 and 1.17, were prepared by anionic polymerization using *s*-BuLi as an initiator in either benzene or hexane at room

^{a)}E-mail: hdiogo@tecnico.ulisboa.pt

^{b)}E-mail: mouraramos@tecnico.ulisboa.pt

temperature in conditions that yield comparable *cis*-contents. The so-obtained average microstructures were 70%/24%/6%, respectively, 78%/14%/8% of *cis/trans*/4,3-addition from H-NMR in CHCl₃ from typical anionically prepared polymers in the investigated range. The polymers were stabilized with butylated hydroxytoluene (0.1%) upon precipitation in methanol. The weight-average molecular weights M_w and weight distributions were determined by either off-line (Chromatix KMX6) in n-heptane or on-line low-angle light scattering (Helios II Wyatt) in tetrahydrofuran from the polydispersity indexes obtained from size-exclusion chromatography. They were in good agreement with values from a universal calibration on the basis of polyisoprene standards. The number average M_n was determined. The molecular weights and polydispersity indexes of the studied samples are listed in Table I. Absolute errors on molecular weights are about 500, respectively, 5000 g mol⁻¹ in the low and high molecular weight.

B. Methods

1. Differential scanning calorimetry (DSC)

The calorimetric measurements were performed with a 2920 MDSC system from TA Instruments, Inc. (USA). The samples of ~5-10 mg were introduced in aluminium pans. The measuring cell was continuously purged with dry high purity helium gas at a flow rate of 30 ml min⁻¹. An empty aluminium pan, identical to that used for the sample, was used as the reference. Cooling was achieved with a liquid nitrogen cooling accessory which permits automatic and continuous programmed sample cooling down to -150 °C. The baseline was calibrated by scanning the temperature domain of the experiments with an empty pan. Additional details on the calibration procedures, including temperature and enthalpy, are given elsewhere.¹⁹

2. TSDC and thermally stimulated polarization currents (TSPC)

Thermally stimulated current experiments were carried out with a TSC/RMA spectrometer (TherMold, USA) covering the range from -170 °C to +400 °C. For these measurements, the sample was placed between the disc-shaped electrodes (7 mm diameter) of a parallel plate capacitor.

The TSDC technique is based on the possibility of producing a stable non-equilibrium dipolar electret by cooling down the sample under the influence of a polarizing *dc* electric field. This is so because the relaxation time of the motional processes increases as temperature decreases, so that it can be rendered

exceedingly long (freezing process) compared with the time-scale of the experiment. The TSDC technique is adequate to probe slow molecular motions (1–3000 s).

The *partial polarization* (PP) procedure, also called fractional polarization (see the Appendix for a short description of a TSDC experiment), is currently used in order to decompose a wide and broad relaxation into narrowly distributed components. Two important parameters in a TSDC experiment are the temperature, T_P , at which the polarizing electric field is turned on, and the temperature $T_P' < T_P$ at which the field is turned off (see Figure 1(a)). If the polarizing field is applied in a narrow temperature interval, i.e., if the difference $T_P - T_P' = \Delta T$ is small, it will probe narrowly distributed relaxation modes (see the Appendix) and, in the limit of a very narrow polarization window, the experimental depolarization current peak is supposed to correspond to an elementary mode of relaxation.²⁰ Let us note that using the partial polarization procedure does not imply the assumption of a discrete distribution of relaxation times. The result of a PP experiment is a peak that does not correspond to a discrete mode of motion, but rather to a narrow slice of the broad continuous distribution. The discussion of the methods for TSDC data treatment and of the nature of the information provided by the TSDC technique is presented elsewhere.^{4,6,20–22}

Another experimental protocol sometimes used in thermally stimulated currents is the so-called polarization mode: we are dealing now with TSPC. The TSPC experiment is schematically represented in Figure 1(b). In this procedure, the sample is submitted to a constant rate heating process in the presence of the polarizing field, and the current intensity, $I(T)$, is recorded while the sample is under short-circuit during

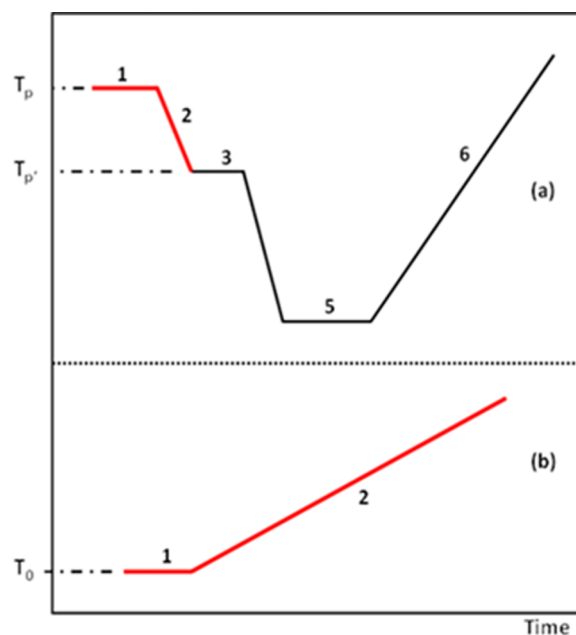


FIG. 1. Experimental protocol, in the form of a temperature-time diagram, for (a) A TSDC experiment. The width of the polarizing window is $\Delta T = T_P - T_P'$ which is typically between 0 and 5 °C in a PP experiment. The electric field is on in steps 1 and 2 (red thicker lines). The depolarization current is measured during the constant rate heating process (step 6). (b) A TSPC experiment. The electric field is on in steps 1 and 2 (red thicker lines). The polarization current is measured during the constant rate heating process (step 2).

TABLE I. Weight averaged molecular weight, M_w , and polydispersity index, *PDI*, of the different PI samples.

| Polymer | M_w | <i>PDI</i> |
|---------|---------|------------|
| 2k | 2 600 | 1.13 |
| 5k | 4 600 | 1.04 |
| 10k | 8 100 | 1.05 |
| 200k | 237 700 | 1.11 |
| 750k | 542 900 | 1.17 |

heating. The charging current has two contributions: the dipolar orientation and the motion of space charges. These contributions behave differently as a function of temperature as will be discussed later.

III. RESULTS AND DISCUSSION

A. Differential scanning calorimetry

Differential scanning calorimetry was used to characterize the calorimetric glass transition signal of the different samples; furthermore, the analysis of the heating rate influence on the temperature location of this signal allows the determination of the activation energy of the structural relaxation, $E_a(T_g)$, and of the steepness (or fragility) index, m , of the glass transformations. The most relevant results are displayed in Table II, and the DSC heat flow curves for the three lower molecular weight samples are shown in the inset of Figure 2.

The influence of the molecular weight on the glass transition temperature, T_g , and on the fragility index, m , will be discussed later, together with the TSDC results.

B. Thermally stimulated currents

In the TSDC thermogram of the lower molecular mass polyisoprenes (2k, 5k, and 10k), two relaxation peaks were found which are shown in Figure 2. It is clear that the two peaks in 2k show a significant degree of overlapping, that both peaks shift to higher temperatures as the molecular weight increases, and that the difference in the temperature location of the two peaks also increases with increasing molecular weight.

These features suggest that the higher temperature peak is the signature of the normal mode relaxation in TSDC.¹⁴ Moreover, from the inset of Figure 2, we see that the higher temperature relaxation does not display any signature in the heat flow curve. The technique of PP was used to decompose the widely distributed global thermogram into single peaks that correspond to narrowly distributed relaxation components. Some results relative to the sample 2k are displayed in Figure 3 that shows different PP depolarization peaks that are the signature of narrowly distributed components of the complex relaxations. Let us briefly note here that several figures displayed to illustrate our experimental results are based on sample 2k data; this is so because the behavior of the other samples is similar except, as discussed later, for the normal mode in the higher molecular weight samples 200k and 750k.

Given that the two relaxations in the sample 2k are overlapped (see Figure 2), Figure 3 illustrates very interestingly the resolution power of the TSDC technique, i.e., the ability

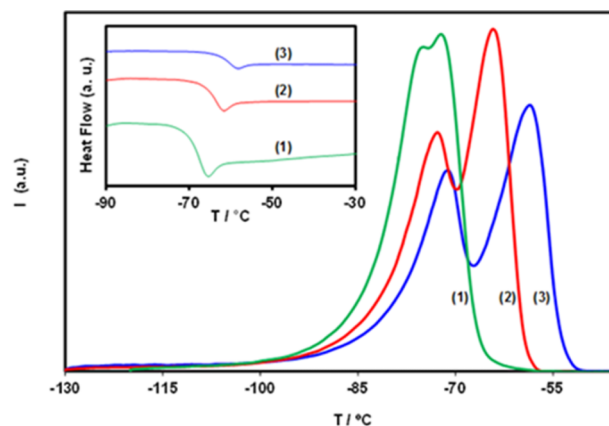


FIG. 2. TSDC thermograms of the three lower molar mass isoprene samples: (1) 2k; (2) 5k; (3) 10k. The results were taken from wide polarization window experiments (see the Appendix) with $\Delta T = 90$ K (between -40 and -130 °C) at a heating rate of 8 °C min^{-1} . The inset shows the DSC heat flow curves (exo up) of the same samples in the region of the glass transition signal, taken at 10 °C min^{-1} on heating.

of the PP procedure for decomposing a complex, broad, and widely distributed relaxation peak into its narrowly distributed components. The peak with higher intensity in the glass transition relaxation (left hand side of Figure 3) has a maximum at $T_{\text{max}} = -76.5$ °C = T_{Mg} , which is the glass transition relaxation provided by the TSDC technique²³ (see Table III below). On the other hand, in the right hand side of Figure 3, the peak with higher intensity in the normal mode relaxation has a maximum at $T_{\text{max}} = -72$ °C = T_{Mn} (see Table IV below).

1. The temperature dependent relaxation time

The standard treatment of each experimental PP peak provides the kinetic information regarding the corresponding motional mode, i.e., the temperature dependent relaxation time, $\tau(T)$ (see supplementary material of Ref. 22 for details). In synthesis, the analysis of the partial polarization results is based on the hypothesis that the depolarization process obeys

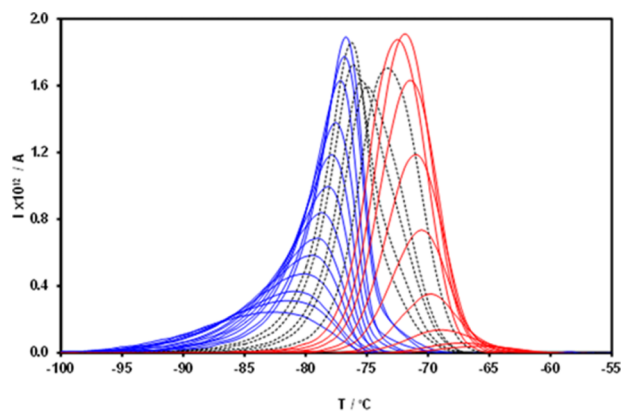


FIG. 3. PP peaks obtained on 2k polyisoprene in the glass transition transformation region and above T_g . In the complex dotted peaks, there is overlap between segmental and chain modes. The polarization temperatures were from $T_P = -88$ °C to -67 °C with intervals of 1 °C. The applied voltage was $V = 400$ V, to a sample of thickness of ~ 0.2 mm; the polarization time, $t_P = 5$ min, the width of the polarization window $\Delta T = 2$ K, and the heating rate $r = 6$ °C min^{-1} .

TABLE II. Onset of the glass transition DSC signal (at 10 °C min^{-1} on heating), $(T_g)_{\text{on}}$, activation energy of the structural relaxation, $E_a(T_g)$, and steepness index, m , of polyisoprene with different molecular weights.

| | 2k | 5k | 10k | 200k | 750k |
|---------------------------------|-----|-----|-----|------|------|
| $(T_g)_{\text{on}} / \text{°C}$ | -71 | -68 | -63 | -61 | -62 |
| $E_a(T_g) / \text{kJ mol}^{-1}$ | 199 | 275 | 249 | 243 | 188 |
| m (DSC) | 51 | 70 | 62 | 60 | 47 |

TABLE III. Kinetic features of the glass transition relaxation provided by TSDC: temperature location of the glass transition peak, T_{Mg} , enthalpy of structural relaxation, $E_a(T_{Mg})$, relaxation time at T_{Mg} , $\tau(T_{Mg})$, and steepness index.

| Sample | 2k | 5k | 10k | 200k | 750k |
|----------------------------------|-------|-----|-----|------|------|
| $T_{Mg}/^{\circ}\text{C}$ | -76.5 | -73 | -71 | -68 | -69 |
| $E_a(T_{Mg})/\text{kJ mol}^{-1}$ | 215 | 226 | 236 | 240 | 240 |
| $\tau(T_{Mg})/\text{s}$ | 16 | 14 | 14 | 14 | 14 |
| $m(\text{TSDC})$ | 55 | 60 | 61 | 62 | 62 |

a first order rate kinetics, i.e., that

$$\frac{dP(t)}{dt} = J(T) = \frac{P(T)}{\tau(T)}, \quad (1)$$

where $P(t)$ is the polarization stored by the sample at time t , $J(T)$ the depolarization current density at temperature T , and $\tau(T)$ is a temperature dependent relaxation time, characteristic of the narrowly distributed component under consideration. This assumption was the subject of controversy, and its correctness was discussed in detail elsewhere.^{7,24} In Eq. (1), temperature and time are related by $dT = r \cdot dt$, where r is the heating rate of the linear heating ramp of the TSDC experiment (step (6) in Figure 1). The temperature dependent relaxation time can be obtained by rewriting Eq. (1) as

$$\tau(T) = \frac{\frac{1}{r} \int_T^{T_f} J(T') dT'}{J(T)} = \frac{\frac{1}{r} \int_T^{T_f} I(T') dT'}{I(T)}, \quad (2)$$

where I is the current intensity, whereas J denotes the current density (the current intensity per unit area). Equation (2) allows the calculation of the relaxation time at each temperature T of the depolarization process given that $J(T)$ is the output of a partial polarization experiment, and $P(T)$ represents the area of the PP peak above the temperature T . This capability of directly calculating the temperature dependent relaxation time from the results of a single PP experiment constitutes an important quantitative feature of the TSDC technique.

The kinetic parameters (apparent activation energy and pre-factor, or activation enthalpy and entropy) are obtained by fitting $\tau(T)$ with a suitable equation (Arrhenius, Eyring, Vogel, WLF, ...). Figure 4 shows the obtained kinetic information in the form of a relaxation map, where the activation energy at the temperature of the maximum intensity, $E_a(T_{\max})$, of the partial polarization peaks shown in Figure 3 is plotted against the temperature location (T_{\max}) of the PP peaks; the dashed line displayed, often called zero entropy line or Starkweather line, describes the behavior of motions with zero activation en-

TABLE IV. Kinetic features of the normal mode relaxation provided by TSDC: temperature location of the normal mode peak, T_{Mn} , activation enthalpy at T_{Mn} , $E_a(T_{Mn})$, relaxation, relaxation time at T_{Mn} , $\tau(T_{Mn})$, steepness index, m .

| Sample | 2k | 5k | 10k | 200k | 750k |
|----------------------------------|-----|-----|-----|------|------|
| $T_{Mn}/^{\circ}\text{C}$ | -72 | -65 | -60 | 36 | 51 |
| $E_a(T_{Mn})/\text{kJ mol}^{-1}$ | 145 | 133 | 128 | 71 | 40 |
| $\tau_n(T_{Mn})/\text{s}$ | 18 | 23 | 25 | 100 | 200 |
| m_n | 42 | 37 | 34 | 13 | 7 |

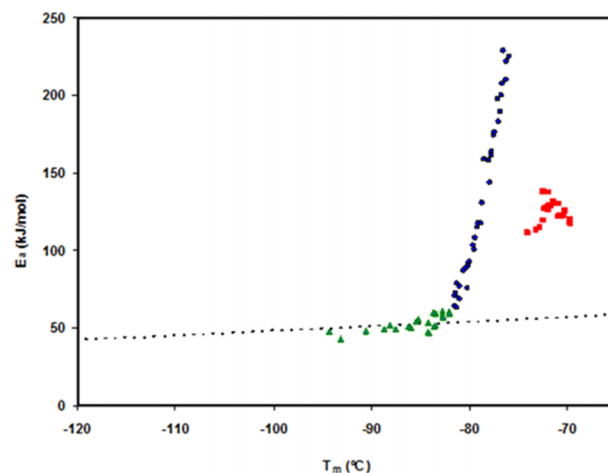


FIG. 4. Relaxation map of polyisoprene 2k: activation energy, E_a , of the partial polarization components of the TSDC spectrum as a function of the temperature of maximum intensity, T_{\max} , of the corresponding current peak. The dashed line is the zero entropy line. Three different kinds of mobility are shown. The triangles belong to the zero entropy line, so that they correspond to local motional modes of the secondary relaxations. The circles show a strong and progressive deviation from the zero entropy line, which is a feature of the glass transition relaxation. The squares correspond to the motional modes of the mobility found above T_g (see Figure 3).

trophy,^{25,26} i.e., the local and non-cooperative motional modes (Arrhenius prefactor $\tau_0 \approx 10^{-13}$ s).

2. The segmental mobility

Figure 4 shows that the relaxation with maximum intensity at -76.5°C in polyisoprene 2k (blue circles) is widely distributed in energy (from 60 to 225 kJ mol^{-1}) and in entropy (from 0 to 800 $\text{J K}^{-1} \text{mol}^{-1}$). The strong deviation from the zero entropy behavior, i.e., the sharp increase with temperature of the activation energy in the glass transformation region, was shown not to arise from the superposition of different Arrhenius-like component processes, but rather to the particular Vogel-Fulcher-Tammann (VFT) temperature dependence of the relaxation time in the temperature range that separates the glassy polymer from the equilibrated polymer melt.²⁷ This is a feature of the glass transition relaxation as studied by TSDC, so that we conclude that this relaxation, located in the proximity of the calorimetric glass transition temperature, is the glass transition relaxation of poly (*cis*-isoprene) 2k as observed by TSDC. Note that the calorimetric T_g values in Table II are ~ 6 K higher compared with the values in Table III obtained by TSDC.

The fragility (or steepness) index of this glass forming polymer can be calculated from TSDC data using the definition

$$m = \left[\frac{d \log_{10} \tau(T)}{d(T_g/T)} \right]_{T=T_g} = \frac{E_a(T_g)}{2.303 \times RT_g}, \quad (3)$$

and considering the highest intensity PP peak in the glass transformation region.^{23,28} For polyisoprene 2k, this higher intensity peak is one of those shown in Figure 3, obtained in a partial polarization experiment with polarization temperature at $T_p = -79^{\circ}\text{C}$, whose temperature location is at $T_M = -76.5^{\circ}\text{C} = T_g$. The Arrhenius activation energy associated to this mode,

calculated at $T_M = T_g$, was found to be $E_a = 215 \text{ J K}^{-1} \text{ mol}^{-1}$, and the fragility index $m = 55$ (see Table III), in reasonable agreement with the value reported before obtained by DSC, and with the values $m = 55$,^{29,30} $m = 57$,³¹ and $m = 62$ ³² reported in the literature. An analysis of the mobility at the glass transformation region, similar to that reported before relative to polyisoprene 2k, has been performed on the other polyisoprene samples, with different molecular weights. The parameters that characterize this molecular mobility for these different polyisoprenes are displayed in Table III.

From Tables II and III, it comes out that the chain length dependence of T_g (from DSC as well as from TSDC) follows the general trend for polymers, i.e., it slightly increases with the molecular weight with a tendency to stabilize at high M_w . This non-continuous behavior with two regimes is believed to arise from the entanglement threshold, M_e , the molecular weight at which entanglements starts in the polymer melt.³³

The influence of M_w on the steepness index of polymers is, contrarily to the influence on T_g , less predictable (see Tables II and III). For example, polyisobutylene is reported to have a fragility that decreases with increasing M_w .³⁴ For most polymers, however, fragility increases as M_w increases (polystyrene, for example, Ref. 35) and a direct correlation between m and M_w such that $m/M_w = \text{cte}$ was proposed,^{33,36,37} based on a study of different polymers. Our results do not seem to fit to such a correlation. Moreover, molecular dynamics simulations for poly(propylene oxide) showed that fragility is independent of the chain length.³⁸ Our fragility values of the structural relaxation obtained by DSC (Table II), as well as those obtained by TSDC (Table III), do not show any apparent trend or correlation with the molecular weight.

3. The chain mobility

The peak observed above T_g in the lower molar mass samples (2k, 5k, and 10k) is a very stable and reproducible peak, that has a temperature location strongly dependent on the molecular weight compared to the glass transition peak (see Figure 2). The peaks in the right hand side of Figure 3, and the squares in the right-hand side of Figure 4, correspond to the narrowly distributed components of this relaxation in polyisoprene 2k (with maximum intensity at $\sim -72^\circ\text{C}$). It comes out from Figure 4 that the temperature dependence of τ for this relaxation is weaker compared to that of the glass transition relaxation. On the other hand, the analysis of the steepness index of this relaxation in the 2k sample, similar to that explained before for the glass transition, leads to the value of $m_n = 42$. It should be noted that the fragility index of a glass forming system is a concept that concerns the glass transition, i.e., the segmental relaxation, and characterizes the strong slowing down of the mobility that occurs as the glass transformation is approached on cooling. However, some authors generalized this concept to other relaxations, and particularly to the normal mode or chain relaxation.³² By analogy to the structural relaxation, the fragility of the normal mode, m_n , is calculated as

$$m_n = \left[\frac{d \log_{10} \tau_n(T)}{d(T_{M_n}/T)} \right]_{T=T_{M_n}} = \frac{E_a(T_{M_n})}{2.303 \times RT_{M_n}}. \quad (4)$$

The value of $m_n = 42$ we obtained from TSDC data for the normal mode of the sample 2k is exactly the same obtained by dielectric relaxation spectroscopy.³² This finding strengthens our previous suggestion that the peak observed by TSDC above the T_g peak indeed corresponds to the normal mode relaxation. An analysis of the mobility above T_g , similar to that reported before relative to polyisoprene 2k, has been also performed on the other polyisoprene samples, with different molecular weights. The main features of the TSDC peaks observed above T_g , in the lower molecular weight samples (2k, 5k, and 10k), i.e., the very high reproducibility of the shape and temperature location, the temperature location strongly dependent on the molecular weight compared to the glass transition peak, and the activation energy lower than that of the structural relaxation,^{15,17,39} strongly suggest that they correspond to the normal mode relaxation rather than to a space charge process.

Let us introduce here a parenthesis to briefly discuss this topic of the nature of the relaxations above T_g , which is important when using thermally stimulated currents. Indeed, the attribution at the molecular level of the TSDC relaxation peaks observed above T_g is often a difficult problem since, as the technique uses *dc* electric fields to polarize the samples, the appearance of artifacts arising from space charge motions is a relatively common occurrence. The space charges present in a dielectric sample, that become mobile above T_g , can be intrinsic (ionic impurities, for example) or extrinsic (normally electrons) created in dielectrics submitted to high fields by injection mechanisms from the electrodes. The electron injection can occur owing to the difference between the ionization energies (work functions) of the metal electrodes and that of the insulator sample. Among the methods used to discriminate between dipolar and space-charge relaxations,^{40,41} we will focus on the one based on the comparison between the TSC results obtained in the depolarization mode (TSDC) and in the polarization mode (TSPC). A dipolar reorientation is a transient process giving rise to a peak, so that a TSPC dipolar peak should be characterized by the same position, height, and shape as the corresponding TSDC peak, the only difference being that the polarization current is of opposite sign. Oppositely, the motion of free carriers is a conduction process which gives rise to a current that steadily increases with temperature, in TSDC as well as in TSPC. On the other hand, in disordered solids, there are charge carriers (homo- and hetero-charges) that move by a hopping mechanism, and can give rise to space charge peaks that can be distinguished from the dipolar peaks by comparing the TSDC and TSPC results. Figure 5 shows results obtained on the sample 2k in both the polarization and the depolarization modes.

In the lower temperature region ($T < -65^\circ\text{C}$), the TSDC and TSPC signals appear as very similar but of opposite signs, so that both peaks at -77°C (glass transition) and -72°C (normal mode) appear to arise from dipolar motions. Above -65°C , the depolarization signals do not show any significant event up to -40°C . On the contrary, the TSPC signals show a complex series of events: the polarization current increases to positive values, passes through a maximum, and decreases becoming negative again at $\sim -40^\circ\text{C}$ appearing as an exponentially increasing (in modulus) conduction current. The

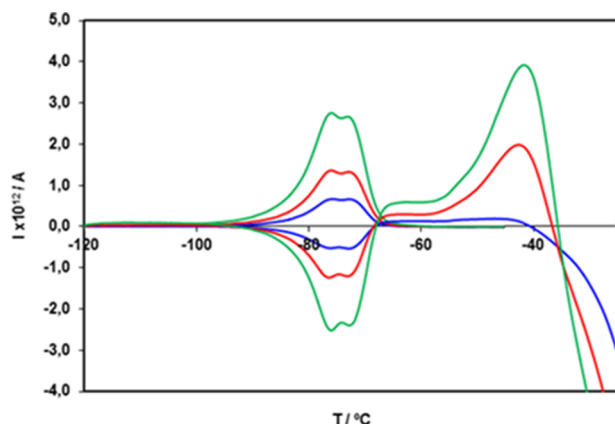


FIG. 5. Evolutions of the TSD current (upper curves) and of the TSP current (lower curves) in polyisoprene 2k. The upper curves are the result of a wide polarization window TSDC experiments with $T_p = 60^\circ\text{C}$ and $T_p' = -125^\circ\text{C}$. The lower curves are the result of a TSPC experiments where the polarizing field was applied in a heating ramp beginning at $T_0 = -120^\circ\text{C}$. The applied voltages were $V = 50, 100$, and 200 V , and the heating rate was $r = 8^\circ\text{C min}^{-1}$ for all the experiments.

behavior shown in the lower temperature region of Figure 5, with a clear symmetry between the TSDC and TSPC traces, was also observed for the 5k and 10k samples. We can thus conclude that this test confirms that the peak above T_g corresponds to a reorientational relaxation process.

The parameters that characterize the chain mobility in the studied samples are displayed in Table IV. For the higher molar mass samples (200k and 750k), the behavior was found to be very different compared with the other samples.

First, since the peak above the glass transition peak is shifted to more than one hundred degrees above T_g (see Tables III and IV), it is hidden in TSPC by strong conduction currents. Furthermore, while the glass transition peak appeared as very reproducible in all the samples, the normal mode peak also showed the same reproducibility in the lower M_w samples, but displayed a significant variability in shape and temperature location in the 200k and 750k samples. Finally, these peaks became very broad as shown in Figure 6 from the comparison between 10k and 750k samples. In fact, the glass transition peaks have identical temperature locations and similar shapes in both samples, but the peaks above T_g are very far apart and have strongly different shapes.

Another feature that comes out from the observation of Table IV is that the activation energy, $E_a(T_{Mn})$, and the fragility index, m_n , of the normal mode decrease smoothly with increasing M_w for the 2k, 5k, and 10k samples, but decrease down to much smaller values for higher M_w samples: $m_n(200k) = 13$ and $m_n(750k) = 7$. We must note that these values are lower than $m = 16$, which is the lower limit of m ,⁴² observed for the glass transition relaxation of extremely strong glass formers, or for simple (local, non-cooperative) viscoelastic relaxations. The differences found in the behavior of the higher M_w samples when compared with the lower M_w ones are probably manifestations of the threshold at the entanglement molecular mass M_e that defines a dynamic crossover characteristic of the normal mode, and was detected and carefully characterized by Adachi et al.^{11,39} The results displayed in Table IV are thus compatible with the finding that the transition between the two regimes

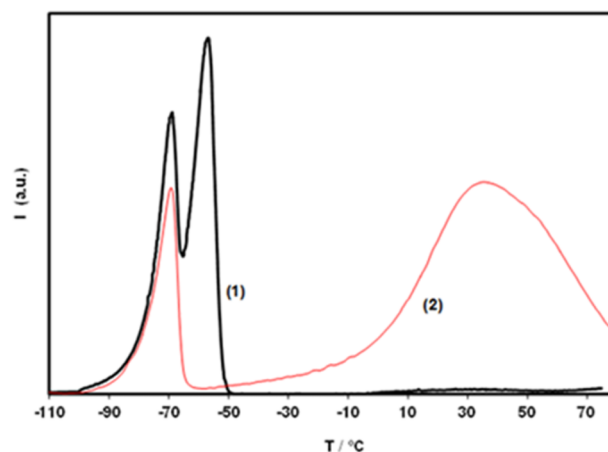


FIG. 6. TSDC thermograms of the 10k ((1), thick line) and 750k ((2), thin line) polyisoprene samples, both recorded at a heating rate $r = 8^\circ\text{C min}^{-1}$. The results were taken from wide polarization window experiments (see the Appendix) with $T_p = 40^\circ\text{C}$ for 10k and $T_p = 75^\circ\text{C}$ for 750k, and $T_p' = -100^\circ\text{C}$ for both experiments.

occurs at $M_w \sim 10\,000\text{ g mol}^{-1}$ for poly (*cis*-1,4-isoprene).³⁹ The stronger decrease of the fragility index of the normal mode above M_e is expected, and is considered as a consequence of both the M_w dependence of τ_n and the temperature dependence of the monomeric friction coefficient. However, the values of $m_n < 16$ have no physical justification since the prefactor of the normal mode is without any doubt smaller than 10^{-13} s . More samples with different molecular weights will be useful to allow a more detailed characterization by TSDC of the transition between the two dynamic regimes.

IV. CONCLUSIONS

From our study by DSC and TSDC of 1,4-*cis*-polyisoprene samples of different molecular weight and low polydispersity, we found that: (i) the fragility index of the structural relaxation determined from DSC and from TSDC results are similar, and in agreement with the literature values obtained by dielectric spectroscopy; (ii) the relaxation peak observed above T_g corresponds to a reorientational process rather than to a space charge motion, so that it can be attributed to the chain relaxation; (iii) the dynamic crossover observed in the normal mode by varying the molecular weight is also revealed in the TSDC results by the temperature location, T_{Mn} , of the normal mode peak, by the values of the relaxation time at T_{Mn} , $\tau(T_{Mn})$, and by the fragility index of the normal mode, m_n . In conclusion, the dielectric technique of thermally stimulated currents appears as a useful and powerful technique in the time domain to study the slow molecular mobility in polymers, confirming and complementing the results obtained from other techniques, namely, the dielectric relaxation spectroscopy.

ACKNOWLEDGMENTS

This work was partially supported by Fundação para a Ciência e a Tecnologia (FCT), Portugal (Projects Pest-OE/CTM/LA0024/2013 and Pest-OE/QUI/UI0100/2013).

APPENDIX: DESCRIPTION OF A TSDC EXPERIMENT

Figure 1(a) schematically shows the steps of a typical TSDC experiment. In the first step, the so-called *polarization step*, the sample is submitted to a *dc* electric field at a given temperature (the *polarization temperature*, T_p), for a given period of time (the *polarization time*, t_p). The applied electric field thus creates in the sample a given amount of polarization. Given that the molecular mobility increases as the temperature increases, at low temperatures, a given electric field only activates simple, local, and non-cooperative dipolar motions while, at higher temperatures, the same electric field is able to polarize more complex motions. In the second step (see Figure 1(a)), the polarized sample is cooled down to a temperature $T_p' = T_p - \Delta T$ in the presence of the electric field. This cooling process allows retaining (at least partially) the polarization created at T_p by the electric field and, at the end of this step (2), with the sample at the temperature T_p' , the polarizing electric field is removed while the sample is left in step (3) for a short period of time (typically 30–60 s). The induced polarization (atomic and electronic), characterized by very short characteristic times, will rapidly disappear at the very first moments of this step, but part of the orientational polarization will remain as the characteristic time of the orientational polarization is longer. The sample so obtained thus presents a given amount of orientational polarization that is stabilized in step (4), by cooling down to a lower temperature T_0 , some tens of degrees lower than T_p' . This possibility of producing a sample with permanent polarization arises from the fact that the relaxation time of the molecular motions is, in general, temperature dependent, in such a way that it increases with decreasing temperature. At the end of step (4) of the TSDC experiment, the sample is thus a stable electret, i.e., a non-equilibrium state in which the depolarization is prevented at T_0 . Finally, in step (6) (see Figure 1(a)), the polarized sample is submitted to a constant rate heating ramp where the sample depolarizes, returning to the equilibrium state, which originates a measurable current intensity, $I(T)$, the transient depolarization current, that is recorded as a function of temperature. The experimental result is a current peak, $I(T)$, whose appearance can be rather complex; this complexity depends on the temperature interval, ΔT , where the polarizing field acts, often referred as *polarization window*. If ΔT is wide ($T_p \gg T_p'$), the polarization at the beginning of the heating ramp (step (6)) includes a wide variety of motional processes, which are depolarized in such a way that less hindered motions depolarize at lower temperatures, while the most hindered motions depolarize at higher temperatures. In contrast, if ΔT is small, the retained polarization arises from a narrow variety of motional modes. Such an experiment with a narrow ΔT is often called *PP* TSDC experiment, and Figure 3 shows results of such kind of experiments.

- ¹W. H. Stockmayer, *Pure Appl. Chem.* **15**, 539 (1967).
- ²N. G. McCrum, B. E. Read, and G. Williams, *Anelastic and Dielectric Effects in Polymeric Solids* (Dover, New York, 1991).
- ³K. Adachi and T. Kotaka, *Prog. Polym. Sci.* **18**, 585 (1993).
- ⁴E. Riande and R. Diaz-Calleja, *Electrical Properties of Polymers* (Marcel Dekker, New York, 2004).
- ⁵*Broadband Dielectric Spectroscopy*, edited by F. Kremer and A. Schön-hals (Springer-Verlag, Berlin/Heidelberg, 2003).
- ⁶B. B. Sauer, *Handbook of Thermal Analysis and Calorimetry*, Vol. 3, edited by S. Z. D. Cheng (Elsevier, Amsterdam, 2002), pp. 653–711.
- ⁷S. S. Pinto, J. J. Moura Ramos, and H. P. Diogo, *Eur. Polym. J.* **45**, 2644 (2009).
- ⁸H. P. Diogo and J. J. Moura Ramos, *IEEE Trans. Dielectr. Electr. Insul.* **21**, 2301 (2014).
- ⁹S. Arrese-Igor, A. Alegría, and J. Colmenero, *Phys. Rev. Lett.* **113**, 078302 (2014).
- ¹⁰S. Arrese-Igor, A. Alegría, and J. Colmenero, *ACS Macro Lett.* **3**, 1215 (2014).
- ¹¹K. Adachi and T. Kotaka, *Macromolecules* **17**, 120 (1984).
- ¹²K. Adachi and T. Kotaka, *Macromolecules* **18**, 466 (1985).
- ¹³Y. Imanishi, K. Adachi, and T. Kotaka, *J. Chem. Phys.* **89**, 7593 (1988).
- ¹⁴D. Boese, F. Kremer, and L. J. Fetters, *Makromol. Chem., Rapid Commun.* **9**, 367 (1988).
- ¹⁵D. Boese and F. Kremer, *Macromolecules* **23**, 829 (1990).
- ¹⁶D. Boese, F. Kremer, and L. J. Fetters, *Macromolecules* **23**, 1826 (1990).
- ¹⁷A. Schön-hals, *Macromolecules* **26**, 1309 (1993).
- ¹⁸A. Schön-hals and E. Schlosser, *Phys. Scr. T* **49A**, 233 (1993).
- ¹⁹J. J. Moura Ramos, R. Taveira-Marques, and H. P. Diogo, *J. Pharm. Sci.* **93**, 1503 (2004).
- ²⁰G. Teyssedre and C. Lacabanne, *J. Phys. D: Appl. Phys.* **28**, 1478 (1995).
- ²¹N. T. Correia, J. J. Moura Ramos, M. Descamps, and G. Collins, *Pharm. Res.* **18**, 1767 (2001).
- ²²J. J. Moura Ramos, N. T. Correia, and H. P. Diogo, *Chem. Educ.* **14**, 175 (2009), available online at <http://chemeducator.org/tocs/t9014004.htm>.
- ²³N. T. Correia, C. Alvarez, and J. J. Moura Ramos, *Polymer* **41**, 8625 (2000).
- ²⁴M. T. Viciosa, G. Pires, and J. J. Moura Ramos, *Chem. Phys.* **359**, 156 (2009).
- ²⁵H. W. Starkweather, *Macromolecules* **14**, 1277 (1981).
- ²⁶J. J. Moura Ramos, *Mol. Phys.* **90**, 235 (1997).
- ²⁷A. Alegría, L. Goitiandia, and J. Colmenero, *J. Polym. Sci., Part B: Polym. Phys.* **38**, 2105 (2000).
- ²⁸J. J. Moura Ramos and N. T. Correia, *Phys. Chem. Chem. Phys.* **3**, 5575 (2001).
- ²⁹A. P. Sokolov and Y. Hayashi, *J. Non-Cryst. Solids* **353**, 3838 (2007).
- ³⁰A. P. Sokolov, V. N. Novikov, and Y. Ding, *J. Phys.: Condens. Matter* **19**, 205116 (2007).
- ³¹S. Pawlus, K. Kunal, L. Hong, and A. P. Sokolov, *Polymer* **49**, 2918 (2008).
- ³²Y. Ding and A. P. Sokolov, *Macromolecules* **39**, 3322 (2006).
- ³³J. Hintermeyer, A. Herrmann, R. Kahlau, C. Goiceanu, and E. A. Rossler, *Macromolecules* **41**, 9335 (2008).
- ³⁴K. Kunal, M. Paluch, C. M. Roland, J. E. Puskas, Y. Chen, and A. P. Sokolov, *J. Polym. Sci., Part B: Polym. Phys.* **46**, 1390 (2008).
- ³⁵C. M. Roland and R. Casalini, *J. Chem. Phys.* **119**, 1838 (2003).
- ³⁶A. A. Elfadl, A. Herrmann, J. Hintermeyer, N. Petzold, V. N. Novikov, and E. A. Rossler, *Macromolecules* **42**, 6816 (2009).
- ³⁷A. Abou Elfadl, R. Kahlau, A. Herrmann, V. N. Novikov, and E. A. Rossler, *Macromolecules* **43**, 3340 (2010).
- ³⁸A. Bormuth, P. Henritzi, and M. Vogel, *Macromolecules* **43**, 8985 (2010).
- ³⁹Y. Imanishi, K. Adachi, and T. Kotaka, *J. Chem. Phys.* **89**, 7585 (1988).
- ⁴⁰J. Vanderschueren and J. Gasiot, in *Topics in Applied Physics*, edited by P. Bräunlich (Springer, Berlin/Heidelberg, 1979), Vol. 37, pp. 135–223.
- ⁴¹S. Devautour, F. Henn, J. C. Giuntini, J. V. Zanchetta, and J. Vanderschueren, *J. Phys. D: Appl. Phys.* **32**, 147 (1999).
- ⁴²R. Böhmer, K. L. Ngai, C. A. Angell, and D. J. Plazek, *J. Chem. Phys.* **99**, 4201 (1993).